 doi:10.20944/preprints202208.0527.v1

Article

Structural Basis for the Binding of Allosteric Activators Leucine and ADP to Mammalian Glutamate Dehydrogenase

Vasily A. Aleshin [1,2], Victoria I. Bunik [1,2,3], Eduardo M. Bruch [4,§], and Marco Bellinzoni [4]

[1] Department of Biokinetics, A. N. Belozersky Institute of Physicochemical Biology, Lomonosov Moscow State University, 119234 Moscow, Russia; aleshin_vasily@mail.ru (V.A.A.); bunik@belozersky.msu.ru (V.I.B.)
[2] Department of Biochemistry, Sechenov University, 119048 Moscow, Russia
[3] Faculty of Bioengineering and Bioinformatics, Lomonosov Moscow State University, 119234 Moscow, Russia
[4] Institut Pasteur, Université Paris Cité, CNRS UMR3528, Unité de Microbiologie Structurale, F-75724 Paris, France; marco.bellinzoni@pasteur.fr (M.B.)
* Correspondence: bunik@belozersky.msu.ru, +7-495-9394484 (V.I.B.), marco.bellinzoni@pasteur.fr, +33-1-45688608 (M.B.);
§ Present address: Sanofi, In vitro Biology, Integrated Drug Discovery, 450 Water st, Cambridge, MA 02141, USA; eduardo.bruch@sanofi.com (E.M.B.).

Abstract: Glutamate dehydrogenase (GDH) plays a key role in the metabolism of glutamate, an important compound at a cross-road of carbon and nitrogen metabolism and a relevant neurotransmitter. Despite being one of the first discovered allosteric enzymes, GDH still poses challenges for structural characterization of its allosteric sites. Only the structures with ADP, and at low (3.5 Å) resolution, are available for mammalian GDH complexes with allosteric activators. Here we aim at deciphering structural basis for the GDH allosteric activation, using bovine GDH as a model. For the first time we report a mammalian GDH structure in a ternary complex with the activators leucine and ADP, co-crystallized with potassium ion. An improved 2.4 Å resolution of the GDH complex with ADP is also presented. The ternary complex with leucine and ADP differs from the binary complex with ADP by the conformation of GDH C-terminus, involved in the leucine binding and subunit interactions. The potassium site, identified in this work, may mediate interactions between the leucine and ADP binding sites. Our data provide novel insights into the mechanisms of GDH activation by leucine and ADP, linked to the enzyme regulation by (de)acetylation.

Keywords: Glutamate dehydrogenase; allosteric regulation; leucine; ADP; potassium; acetylation; thiamine triphosphate

1. Introduction

Mammalian glutamate dehydrogenase (GDH) is an indispensable metabolic enzyme, particularly relevant for the metabolism of the neurotransmitter glutamate in the brain. Mammalian NAD(P)-dependent GDH of 55 kDa (EC: 1.4.1.3) is significantly different from the pathway-specific NAD- (EC: 1.4.1.2) or NADP-dependent (EC: 1.4.1.4) GDH of non-mammalian species. For example, in *Neurospora crassa*, a NADP-dependent GDH is involved in anabolic processes, while a NAD-dependent GDH functions in glutamate catabolism [1,2]. Nevertheless, with an exception of the family of large 180 kDa GDH [3], most of the NAD- or NADP-specific GDH are homologous to mammalian GDH. The latter enzymes are hexameric, organized as a dimer of trimers (Figure 1), possibly forming complexes/aggregates of higher molecular weight [4,5].

Preprints (www.preprints.org) | NOT PEER-REVIEWED | Posted: 31 August 2022 doi:10.20944/preprints202208.0527.v1

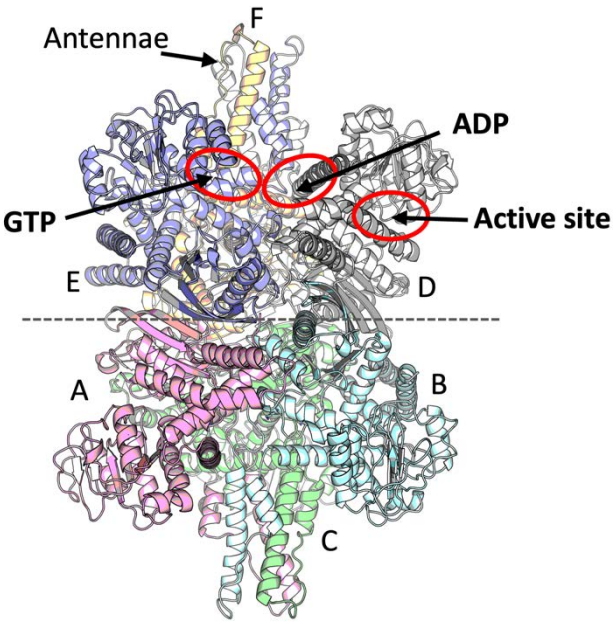

Figure 1. A mammalian GDH model and its ligand binding sites. The six subunits are shown in different colors, while the hexamer is organized as two trimers related by a two-fold axis indicated by a dashed horizontal line. Chains corresponding to 8AR7 and 8AR8 structures are indicated on the graph, showing A, B, C or D, E, F chains to form the two opposite trimers of the GDH hexamer in these models. Two antennae regions are located at the top and bottom of the hexamer, built by three subunits each. Red ovals indicate the active site, ADP activatory and GTP inhibitory allosteric sites.

Mammalian GDH is one of the first allosteric enzymes discovered [6]; its allosteric inhibition by GTP and activation by ADP have been known for more than half-a-century, but the structures of respective complexes have been characterized only recently [7,8]. Both ligands possess separate allosteric binding sites (Figure 1). The activation of mammalian GDH by L-leucine and some other hydrophobic amino acids has also been long known [4], yet no structure of the mammalian GDH with leucine has been obtained up to date.

Despite more than 20 of mammalian GDH structures available in PDB, most of the ligand-binding complexes beyond those with the inhibitor GTP are of low resolution. For example, the only two available structures with the GDH activator ADP are at 3.5 Å resolution and, most likely, arise from the same diffraction data, which limits the mechanistic understanding of the GDH regulation. The differences in resolution appear to correspond to the two major conformational states of the enzyme. That is, an open form (in particular, inherent in the apoenzyme or its complex with ADP) has so far been crystallized at medium to low resolution, whereas higher resolution data had been obtained for the closed form (exemplified by complexes with GTP and some apoenzyme structures or complexes with other ligands). The aim of this work is to improve structural characterization of GDH in its open form. We hypothesize that this may be achieved through synergistic action of the GDH allosteric activators, such as ADP [9], leucine [10] and thiamine triphosphate (ThTP) [11], upon their simultaneous presence in crystallization buffer. Indeed, under such conditions, novel structures of GDH with its activators have been resolved, using GDH from bovine liver as a model of the mammalian GDH family.

We report here the identification of the leucine binding site in a novel ternary complex of mammalian GDH with leucine and ADP at 2.44 Å resolution, and the improved characterization of the GDH complex with ADP at the resolution of 2.4 Å. The

Preprints (www.preprints.org) | NOT PEER-REVIEWED | Posted: 31 August 2022 doi:10.20944/preprints202208.0527.v1

structures are compared to the known complexes of GDH from different species. In addition, a potassium-binding center is localized, that interacts with both the leucine and ADP sites. The results strongly improve understanding of mammalian GDH regulation by allosteric activators and acetylation of the corresponding allosteric sites.

2. Results

To enhance the resolution of crystallized GDH complexes with its allosteric activators ADP, ThTP and leucine, we assumed that the enzyme active state may be stabilized by simultaneous presence of the activators, as each of the activators may contribute to shifting the enzyme conformational ensemble to the open conformation. Hence, we undertook crystallization trials using the activator combinations, in addition to the conditions comprising single activators. As a result, novel binary and ternary complexes of the enzyme with ADP and leucine are crystallized in the media with ThTP, even though ThTP is not identified as a bound ligand in any of the collected datasets.

2.1. Identification of the leucine binding site of mammalian GDH

For the first time, the structure of a mammalian GDH in a ternary complex with ADP and leucine is solved (Table 1), showing the structural basis of leucine regulation (Figure 2A). Crystals of bovine GDH in complex with leucine and ADP (PDB ID: 8AR7) and with ADP alone (PDB ID: 8AR8) were obtained from the protein solution supplemented with the activators, ThTP included.

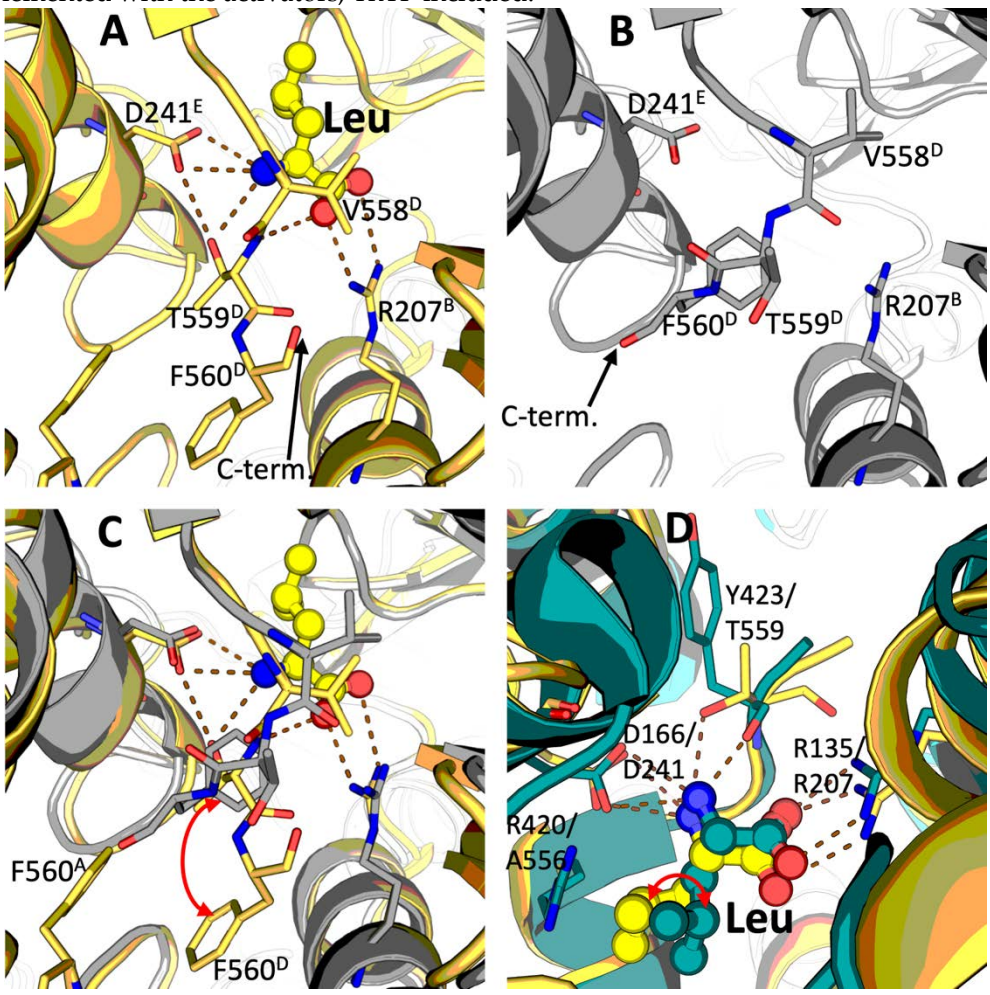

Figure 2. Binding of leucine by bovine GDH. A – structure of leucine (Leu) binding site in the ternary GDH complex with leucine and ADP – PDB 8AR7 (the cartoon and carbon atoms are in yellow, dashed lines indicate the H-bonds); B – structure of leucine binding site in the binary

Preprints (www.preprints.org) | NOT PEER-REVIEWED | Posted: 31 August 2022 doi:10.20944/preprints202208.0527.v1

complex of GDH with ADP – PDB 8AR8 (the cartoon and carbon atoms are in gray). The leucine binding site is shown at the interface of chains B, D and E of the GDH hexamer, as defined in Figure 1. The chain D is traced till residue F560 in both complexes; in the binary GDH·ADP complex, the GDH C-terminal end assumes an equivalent conformation to the one observed in other GDH structures in the open form (e.g., PDB 3JCZ or 7VDA [12,13]). C – Conformational changes in the leucine binding site upon binding of the activator (images (A) and (B) are superposed, with the main shift of F560 indicated by the red arrow); D – comparison of the leucine binding sites in the bovine (yellow) and *T. thermophilus* (teal) GDH structures. The different conformation of the leucine side chain in the complexes of bacterial and mammalian GDH is indicated by the red arrow. Chain A of PDB 3AOE (gdhB) is used for the bacterial GDH model. The conformation of bound leucine in other subunits, including those encoded by *gdhA*, is similar [14].

A bound leucine molecule was observed in all the six equivalent sites within the mammalian GDH hexamer. Leucine binds at the contact area between the three different subunits, involving those from the opposite trimers forming the GDH hexamer (Figure 1 and 2). While the R207^{B} guanidinium group makes a salt bridge with the leucine carboxyl group, the D241^{E} carboxyl group from another subunit binds the leucine amino group, which in turn interacts also with the hydroxyl group of T559^{D} located at the C-terminal end of the third subunit. Simultaneously, the main chain amide group of the same T559^{D} is hydrogen-bonded to one of the leucine carboxyl oxygens (Figure 2A). Additionally, the hydroxyl group of T559^{D} acts as an H-bond donor to D241^{E}, contributing to orienting it properly towards the bound leucine. Leucine may thus enable signal transduction between GDH subunits, stabilizing interactions within one and between the opposite trimers (Figure 1 & 2). Remarkably, while the side chains of D241^{E} and R207^{B} occupy the same location in the absence of leucine (Figure 2B), the conformational change induced by leucine binding essentially involves the C-terminal segment of GDH, mostly disordered in the absence of leucine (where it can be traced for chain D only), with T559^{D} providing key contacts to the leucine activator and, at the same time, interacting with R207^{B} (Figure 2A-C). That is, upon leucine binding residues V558^{D}, T559^{D} and F560^{D} move significantly, with T559^{D} flipping and its side chain replacing the phenyl group of F560^{D} to interact with the bound leucine. However, the novel conformation assumed by the aromatic side chain of F560^{D}, following the ~ 4 Å displacement down upon leucine binding, makes it involved in stacking interactions with the equivalent F560^{A} from a different GDH subunit belonging to the opposite trimer (Figure 2A). Overall, these interactions suggest that leucine binding promotes and stabilizes the interactions within and between the GDH trimers at once (Figure 1 and 2C). The considered interactions of the bound leucine are equivalent in all the six leucine binding sites present in the GDH hexamer.

Noteworthy, the leucine binding pocket identified by us in the homohexameric bovine GDH, is similar to the one observed in heterohexameric GDH from *Thermus thermophilus* (PDB 3AOE, [14,15]) (Figure 2D). The main residues responsible for binding the leucine carboxyl and amino groups are conserved, *i.e.* R135 and D166 from *T. thermophilus* GDH are structurally equivalent to R207 and D241 in bovine GDH. However, the conformation of the side chain of the bound leucine differs between the bacterial and bovine GDH, most likely as a result of the presence of a bulkier side chain in the C-terminal segment in both subunits of bacterial heterohexamer (R415 in gdhA, R420 in gdhB), absent in the bovine enzyme where the equivalent residue is A556 (Figure 2D). Interestingly, although bovine T559 is not conserved, replaced in *T. thermophilus* by a proline (C-terminal residue both in gdhA and gdhB), the H-bond to the leucine amino group is provided in *T. thermophilus* by the carbonyl oxygen of the preceding tyrosine (either Y418 or Y423 in gdhA or gdhB, respectively), which occupies the equivalent place (Figure 2D).

Thus, our GDH structure, crystallized with leucine and ADP, enables novel understanding of the mechanisms of leucine binding to GDH of mammals.

 doi:10.20944/preprints202208.0527.v1

2.2. Novel conformation of GDH·ADP binary complex at 2.4 Å resolution

Resolution of both the ternary GDH·ADP·Leu (2.44 Å) and binary GDH·ADP (2.4 Å) complexes strongly exceeds that of the GDH·ADP structures previously reported (3.5 Å). Our data reveal no significant difference in the bound ADP conformation between the GDH·ADP·Leu and GDH·ADP complexes.

Of the two GDH structures with ADP available in PDB, namely 1NQT and 6DHK, the 6DHK model (deposited in 2018) is linked to the original paper from 2003 [8], describing the older entry 1NQT by the same authors. We therefore use the coordinates from the more recent 6DHK entry as a reference for the comparison to the higher resolution (2.4 Å) GDH·ADP binary complex described here (Table 1). Electron density maps in our resolved binary complex unambiguously reveal the bound ADP and the residues involved in ADP binding, such as R519 interacting with the ADP β-phosphate (Figure 3A *vs* 3B). The overall conformation of the 8AR8 GDH·ADP complex is very close to 6DHK (the two complexes superimpose with an RMSD of ~ 0.6 Å). However, the conformation of the ADP ribose ring differs, revealing a C2′-endo pucker conformation in our structure (Figure 3A), while the same was ascribed either the C2′-endo or C3′-endo conformation in 6DHK (Figure 3B). With the higher resolution achieved in our case, the H-bonding between the carboxyl group of D179 and the 2′-hydroxyl of ADP become obvious (Figure 3A). In addition, due to the ADP ribose C2′-endo pucker conformation, we could not observe any interaction between the ADP 2′-hydroxyl and R551, in contrast to the previous models (Figure 3B).

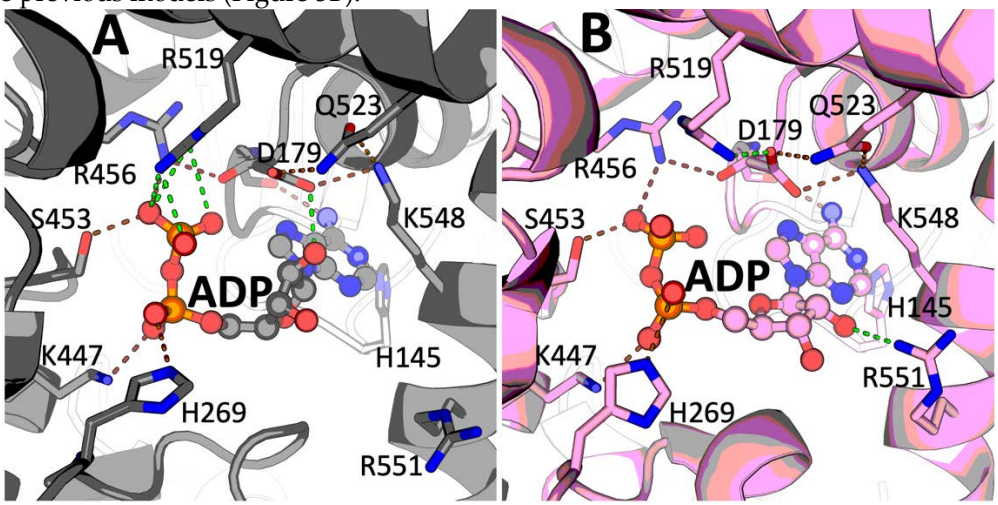

Figure 3. Comparison of ADP binding in the new GDH·ADP complex of 2.4 Å resolution (A) and previously reported complex 6DHK (B). A – the C2′-endo conformation of the ADP in the 8AR8 structure, shown in gray. B – the C3′-endo conformation of the ADP in the 6DHK (3.5 Å resolution) structure, shown in pink. Similar ADP bonds in both structures are shown by brown dashed lines, the green lines indicate the differences between the 8AR8 and 6DHK entries.

Thus, our data resolve significant details on ADP conformation bound in the allosteric site of a mammalian GDH.

2.3. Identification of the GDH binding site for potassium ion.

The ternary complex of mammalian GDH with ADP and leucine (8AR7) also shows a potassium ion (K^+) bound in each GDH subunit (Figure 4A). K^+ is identified as the most likely bound ion from those added to the crystallization mixture (2 mM potassium ADP and 500 mM NaCl), by careful analysis of the electron density, nature and interatomic distances to protein atoms. The presence of orders of magnitude higher concentration of Na^+ (500 mM) *vs* K^+ (2 mM) in the protein buffer suggests a specificity for K^+ in this site, which has not been reported so far for a mammalian GDH. Noteworthy, no ion could be

Preprints (www.preprints.org) | NOT PEER-REVIEWED | Posted: 31 August 2022 doi:10.20944/preprints202208.0527.v1

observed in this site in the binary GDH·ADP complex, which contained Ca^{2+} (20 mM) in addition to K^+ (2 mM) and Na^+ (500 mM) in the crystallization buffer (as described in chapters 4.1 and 4.2 of "Materials and Methods"). Instead, the electron density maps for the binary GDH·ADP complex rather suggest the presence in this site of a tightly bound water molecule, as modelled (Figure 4B), or alternatively a Na^+ ion.

The K^+ binding site is located at the end of the α-helix which ends with P114, and is formed by the main chain carbonyl atoms of I111, I112, P114 and H142, and the carboxamide oxygen of N116 (Figure 4). The α-helix near the cation-binding site interacts with the C-terminal GDH helix (Figure 4C). Taking into account the significant involvement of the C- terminus of the enzyme in leucine binding, the substitution of the water molecule in the GDH·ADP complex by a potassium ion in the GDH·ADP·Leu complex may be due to the leucine-induced rearrangement of the C-terminal GDH part. Remarkably, H142 participates directly in the K^+-site formation through its main chain oxygen, while S143 links the cation to the ADP site through H145, whose imidazole side chain in turn H-bonds both to S143 and to the ADP adenine ring (Figure 4D). In addition, a water molecule from the K^+ coordination sphere is H-bonded to the hydroxyl group of Y553, which side chain makes Van der Walls interactions with the bound leucine (Figure 4A). Hence, the newly identified K^+-binding may stabilize the open conformation of the enzyme in the ternary GDH·ADP·Leu complex, transducing signals between the ADP and leucine sites. Our structural data suggest that the affinity to K^+ may be significantly decreased in the binary GDH·ADP complex.

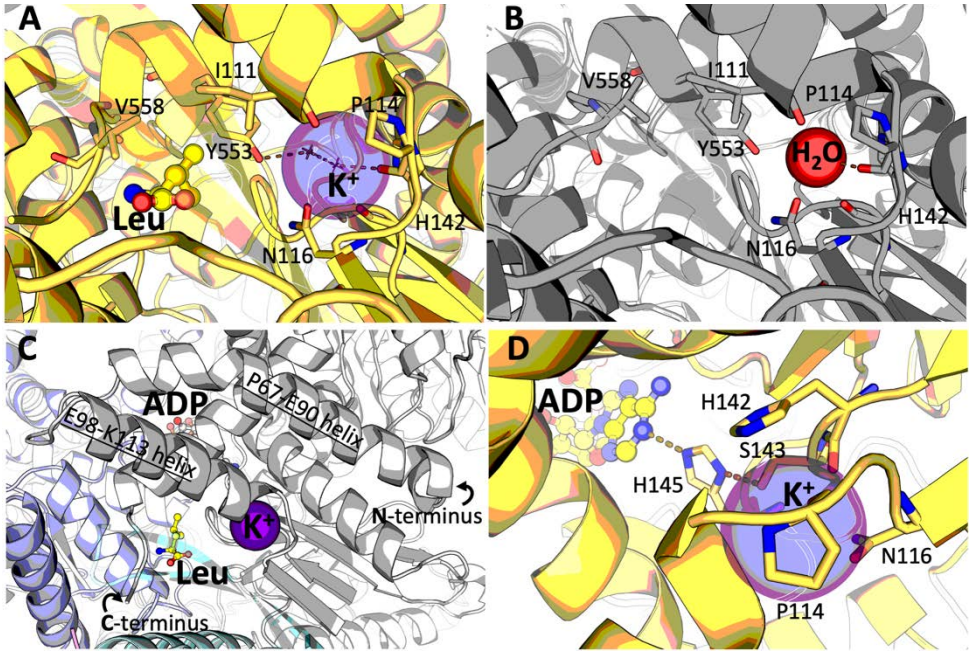

Figure 4. K^+-binding site in mammalian GDH. A – The K^+ binding in the GDH·ADP·Leu complex colored as in Figure 2A. The interaction of K^+ and leucine through Y553 and a water molecule from the coordination sphere of K^+ is shown; B – The same site in the GDH·ADP complex (colored as in Figure 2B), where the potassium ion is modelled to be substituted by water; C – Relative positions of the leucine, ADP and potassium binding sites at the interface of GDH trimers, colored as in Figure 1; D – Interaction between the K^+- and ADP-binding sites. The ADP binding modes are equivalent in both the GDH·ADP·Leu and the GDH·ADP complexes described here. H-bonds are shown as dashed lines. All indicated residues belong to one chain.

3. Discussion

We report here new structures of mammalian GDH complexes with the allosteric activators ADP and leucine, which show the open form of the enzyme under significantly increased (down to 2.4 Å) resolution, compared to the previously known structures of the

 doi:10.20944/preprints202208.0527.v1

GDH open form with ADP (3.5 Å). While structures of bacterial or fungal GDHs have been deposited at resolutions down to 1.7 Å (PDB 5GUD and 7ECR) [16,17], the lower resolution of mammalian GDH in X-ray crystallography seems to correlate with the presence of a 50-residue "antenna" domain, participating in allosteric regulation. Although single particle cryo-electron microscopy (cryo-EM) has been used to overcome these limitations and provided bovine GDH models at resolutions down to 1.8 Å (PDB 5K12, which is however missing most of the NAD(P)(H) binding domains and significant parts of the N- and C-terminal ends [18]), the complexes of mammalian GDH with either GTP or NADH solved so far by cryo-EM have not yet contributed significant new insights, in part because of their resolutions still not exceeding 3.3 Å [12].

3.1. Leucine binding site

The GDH·ADP·Leu ternary complex resolved in this work represents the first structure of the leucine allosteric site in mammalian GDH. The only previously reported structure of this allosteric site used a 50 kDa GDH from *T. thermophilus*, a Gram-negative thermophile bacterium possessing a GDH heterohexamer formed by four gdhA and two gdhB subunits [14,15]. Such heteromeric organization of GDH, where one type of the subunits is catalytically inactive and acts as the regulatory subunit for activation by leucine (gdhA) [19], is not known in mammals. Additionally, the GDH from *T. thermophilus* does not bind ADP, but instead may be activated by AMP within its heterocomplex with the product of the gene *TTC1249*, proposed to act as an AMP-sensory subunit [19]. Despite these significant differences in the GDH regulation, the leucine binding sites of bovine and *T. thermophilus* GDH are very similar, suggesting a significant conservation of the allosteric activation mechanisms of GDH through evolution.

Remarkably, the site-directed mutagenesis of human GDH2 has revealed that R151M and D185A mutants, substituted in positions equivalent to the bovine GDH R207 and D241 that are essential for leucine binding (Figure 2), are not activated by leucine [14]. These findings are consistent with our structural data, confirming functional significance of the mammalian GDH residues interacting with leucine at the allosteric site.

3.2. Potassium ion binding site

The mammalian GDH K^+ binding site described here is structurally equivalent to the K^+ site identified in GDH1 from *Arabidopsis thaliana* (6YEH; [20]), and to one of the multiple Na^+-binding sites in the structure of human GDH2 (6G2U; [21]) (Figure 4). Among bacterial GDH with the resolved structures, only GDH from *Corynebacterium glutamicum* contains multiple sites for potassium ion binding (5GUD; [16]), one of them coinciding with the K^+ site of mammalian GDH identified by us. Although such distribution among different species implies the conservation of this cation binding site, determining the nature of the bound ion and its role under physiological conditions across different species will require further investigations. In this respect, our structural data provide hints about a high specificity of this site to potassium ion: In the ternary GDH·ADP·Leu complex, K^+ is observed to bind in the presence of a 250-fold molar excess of Na^+. In addition, the data also suggests a role of the bound ion in stabilizing the open conformation of GDH once activated by leucine, as suggested by the absence of detectable K^+ binding in the GDH·ADP complex. In view of the known complexity and potential synergism of the regulatory action of monovalent and divalent cations [22], identification of a specific K^+ site may add new mechanistic insights to the data on GDH regulation by Zn^{2+} in mammals [23-25] or by Ca^{2+} in plants [20].

3.3. Insights in ADP and leucine binding implications for the GDH regulation by acetylation

 doi:10.20944/preprints202208.0527.v1

Despite the available structural data on mammalian GDH, our understanding of functional significance of post-translational acylation of multiple lysine residues of GDH remains limited. Similarly to the recently shown regulation of the rat brain GDH inhibition by GTP through acetylation of K503 in the allosteric GTP site [26], other known acylation may be involved in regulation of allosteric effects of ADP and leucine. New structural insights in the binding of these GDH activators provide for a better understanding of the acylation-imposed regulation of the allosteric effects. Of the residues involved in ADP binding by bovine GDH, K548 (Figure 3) corresponds to human/mouse K545, known to be acetylated [27,28]. Changing the ε-amino group charge and steric constraints, acetylation of bovine K548, which helps orienting D179 for its interaction with the 2'-hydroxyl of ADP (Figure 3A), should decrease ADP binding affinity.

Of lysine residues in the proximity of newly identified leucine binding site, K203 that is located close to the C-terminal end of GDH, corresponds to the acetylatable human/mouse K200 [27,28], with the K203 acetylation possibly affecting allosteric action of leucine through changed conformational mobility of the GDH C-terminus (Figure 2).

Thus, localization of the leucine site and improved understanding of the ADP binding provide new information for unraveling functional consequences of the independently identified acylations of the GDH lysine residues.

3.4. Binding of thiamine derivatives

Although both GDH complexes described here have been obtained in the presence of ThTP, which is a known activator of GDH [11], no bound ThTP could be detected in our crystals. The failure to see ThTP bound to GDH may be ascribed to several factors, not last the long time required to grow suitable bovine GDH crystals, causing ThTP hydrolysis and/or degradation due to the thiazolium ring opening at pH > 7. Nevertheless, it is worth noting that both crystal forms of GDH in its active open form, obtained here in the presence of ThTP, have not been reported before, neither could the properly diffracting samples be obtained in our crystallization mixtures in the absence of ThTP, or with ThTP replaced by thiamine diphosphate. Our observations therefore favor a contribution of ThTP to the conformational stabilization of the activated form of GDH during crystallization, warranting further studies of the thiamine-dependent regulation of the GDH reaction tightly linked to the thiamine-dependent mitochondrial dehydrogenases of 2-oxoacids.

4. Materials and Methods

4.1. Reagents

Bovine GDH (Merck, G7882) was purchased as lyophilized powder, dissolved in 50 mM HEPES with 500 mM NaCl solution, pH 7, and used for crystallization as it is at 30 mg/ml concentration. ADP (Merck, A5285) was used in the form of monopotassium salt (K·ADP). L-leucine (Merck, L8000) was used. ThTP was synthesized according to the previously published procedure [29] and its purity was checked by NMR. The buffers, salts and other reagents were from Merck.

4.2. Crystallization and data collection

Crystallization was carried out as screenings at 4°C temperature using the sitting-drop vapor diffusion method and a Mosquito nanoliter-dispensing crystallization robot (TTP Labtech), according to established protocols at the Institut Pasteur Crystallography Facility [30]. Crystals appeared after variable times (1 to 2 months). Optimized conditions for crystal growth of the different protein complexes are as follows: (GDH·ADP·Leu): 20% EtOH, 30% 2-methyl2,4-pentanediol (MPD), with a GDH solution (30 mg/ml) supplemented with 2 mM monopotassium ADP, 2 mM trisodium ThTP and 10 mM L- leucine (pH 7); (GDH·ADP): 20 mM $CaCl_2$, 100 mM Na-acetate buffer

 doi:10.20944/preprints202208.0527.v1

(pH 4.6), 30% MPD, with a GDH solution (30 mg/ml) supplemented with 2 mM trisodium ThTP and 2 mM monopotassium ADP. Since both crystallization conditions contain 30% MPD, crystals were frozen in liquid nitrogen without addition of cryoprotectants. X-ray diffraction data were collected from single crystals at 100 K using synchrotron radiation at the beamline ID30B (ESRF, Grenoble, France).

4.3. Structure determination and refinement

The data were processed with XDS [31] run through autoPROC [32], and were scaled with STARANISO provided within the same software, to properly account for diffraction anisotropy. The structures were solved by molecular replacement through the program PHASER [33]. Coordinates of bovine GDH [PDB: 3JCZ] in unliganded open form (from single particle cryo-EM [12]) were used as the search model to first solve the structure of GDH in apo form, which, in turn, served as the molecular replacement search model for the following datasets. Manual rebuilding, ligand pose and adjustments of the models were performed with COOT [34]. Refinement was carried out with BUSTER, applying local structure similarity restraints for noncrystallography symmetry [35] and a Translation–Libration–Screw (TLS) model. Validation of models was performed with MolProbity [36] and the validation tools in PHENIX [37]. A summary of data collection and refinement statistics is provided in Table 1. Graphical representations were rendered with PyMOL 2.5.0 (Schrödinger LLC).

Table 1. Summary of the X-ray data.

	GDH·ADP·Leu	**GDH·ADP**
Synchrotron beamline	ESRF ID30B	ESRF ID30B
Space group	$P2_1$	P1
Unit-cell parameters		
a, b, c (Å)	90.88, 178.71, 123.88	87.51, 92.03, 119.57
α, β, γ (°)	90, 104.00, 90	99.35, 106.73, 109.73
Resolution range (Å)	120.20 – 2.45	47.46 – 2.40
	(2.79 – 2.45)	(2.48 – 2.40)
Wavelength (Å)	0.9763	0.9763
No. measured reflections	445692	331373
No. unique reflections	82997	96056
Multiplicity	5.4 (5.7)	3.4 (3.6)
Completeness (%)	92.0 (60.9)	89.9 (86.0)
Average I/σ(I)	6.8 (1.8)	5.0 (2.0)
Rpim[a]	0.094 (0.551)	0.175 (0.398)
CC(1/2)	0.989 (0.407)	0.925 (0.668)
Refinement statistics		
R_{work}[b] (%)	19.2	20.4
R_{free}[b] (%)	21.4	23.6
No. of non-H atoms		
Macromolecule	22994	22937
Ligands/ions	222	162
Water molecules	439	1019
Average B-factors	68.9	41.4
Rms deviations[c]		

 doi:10.20944/preprints202208.0527.v1

Bonds (Å)	0.010	0.010
Angles (°)	1.37	1.27
Molprobity statistics		
Clashscore	4.26	4.30
Ramachandran outliers (%)	0.07	0.00
Ramachandran favoured (%)	97.41	98.6
Rotamer outliers (%)	3.24	3.61
C-beta deviations	0	1
PDB entry code	8AR7	8AR8

Resolution limits were determined by applying an anisotropic cut-off via STARANISO, part of the autoPROC data processing software [32]; data in parenthesis refer to the highest resolution shell.

[a]$R_{pim} = \Sigma_{hkl}[1/(N-1)]^{1/2}\Sigma_i|I_i(hkl) - \langle I\rangle(hkl)|/\Sigma_{hkl}\,\Sigma_i\,I_i(hkl)$, where N is the multiplicity, I_i is the intensity of reflection i and $\langle I\rangle(hkl)$ is the mean intensity of all symmetry-related reflections [38].

[b]$R_{work} = \Sigma||F_o| - |F_c||/\Sigma|F_o|$, where F_o and F_c are the observed and calculated structure factor amplitudes. Five percent of the reflections were reserved for the calculation of R_{free}.

[c]Calculated with MolProbity [36] within the autoBUSTER refinement suite.

Author Contributions: Conceptualization, V.I.B.; methodology, formal analysis, investigation, and resources, V.A.A., V.I.B., E.M.B. and M.B.; validation and data curation, M.B.; writing—original draft preparation, V.A.A.; writing—review and editing, V.A.A., V.I.B. and M.B.; visualization, V.A.A.; supervision, V.I.B., E.M.B. and M.B.; project administration, V.I.B. and M.B.; funding acquisition, V.A.A., V.I.B. and M.B. All authors have read and agreed to the published version of the manuscript.

Funding: This research was supported by an Ostrogradski fellowship from the French Embassy in Moscow for a PhD international mobility to V.A.A., institutional funding from the Institut Pasteur and the CNRS, and a RSF grant to V.I.B. (grant no. 18-14-00116).

Institutional Review Board Statement: Not applicable.

Informed Consent Statement: Not applicable.

Data Availability Statement: The atomic coordinates and structure factors of the two crystal structures were deposited in the PDB with codes 8AR7 (GDH·ADP·Leu) and 8AR8 (GDH·ADP). All other data needed for evaluation of the conclusions are present in the paper.

Acknowledgments: The authors express their gratitude to Ahmed Haouz, Patrick Weber and Cédric Pissis (Crystallography Platform, Institut Pasteur, Paris) for performing robot-driven crystallization assays, and to Alexey V. Kazantsev (Chemical Faculty of Lomonosov Moscow State University, MSU, Moscow, Russia) for the NMR assay of ThTP purity. The authors also thank the ESRF (Grenoble, France) for granting access to macromolecular crystallography beamlines.

Conflicts of Interest: The authors declare no conflict of interest. The funding sponsors had no role in the design of the study, as well as in the collection, analyses or interpretation of data, the writing of the manuscript or in the decision to publish the results.

Abbreviations

GDH—glutamate dehydrogenase
ThTP—thiamine triphosphate
MPD—2-methyl2,4-pentanediol
Cryo-EM—cryo-electron microscopy

References

1. Barratt, R.W.; Strickland, W.N. Purification and characterization of a TPN-specific glutamic acid dehydrogenase from Neurospora crassa. *Archives of biochemistry and biophysics* **1963**, *102*, 66-76, doi:10.1016/0003-9861(63)90321-7.
2. Veronese, F.M.; Nyc, J.F.; Degani, Y.; Brown, D.M.; Smith, E.L. Nicotinamide Adenine Dinucleotide-specific Glutamate Dehydrogenase of Neurospora. *Journal of Biological Chemistry* **1974**, *249*, 7922-7928, doi:10.1016/s0021-9258(19)42053-x.
3. Lázaro, M.; Melero, R.; Huet, C.; López-Alonso, J.P.; Delgado, S.; Dodu, A.; Bruch, E.M.; Abriata, L.A.; Alzari, P.M.; Valle, M., et al. 3D architecture and structural flexibility revealed in the subfamily of large glutamate dehydrogenases by a mycobacterial enzyme. *Communications Biology* **2021**, *4*, doi:10.1038/s42003-021-02222-x.
4. Yielding, K.L.; Tomkins, G.M. An Effect of L-Leucine and Other Essential Amino Acids on the Structure and Activity of Glutamic Dehydrogenase. *Proceedings of the National Academy of Sciences* **1961**, *47*, 983-989, doi:10.1073/pnas.47.7.983.
5. Frieden, C. The Effect of pH and Other Variables on the Dissociation of Beef Liver Glutamic Dehydrogenase. *Journal of Biological Chemistry* **1962**, *237*, 2396-2400, doi:10.1016/s0021-9258(19)63451-4.
6. Talal, N.; Tomkins, G.M. Allosteric Properties of Glutamate Dehydrogenases from Different Sources. *Science* **1964**, *146*, 1309-1311, doi:10.1126/science.146.3649.1309.
7. Peterson, P.E.; Smith, T.J. The structure of bovine glutamate dehydrogenase provides insights into the mechanism of allostery. *Structure* **1999**, *7*, 769-782, doi:10.1016/s0969-2126(99)80101-4.
8. Banerjee, S.; Schmidt, T.; Fang, J.; Stanley, C.A.; Smith, T.J. Structural studies on ADP activation of mammalian glutamate dehydrogenase and the evolution of regulation. *Biochemistry* **2003**, *42*, 3446-3456, doi:10.1021/bi0206917.
9. Bailey, J.; Bell, E.T.; Bell, J.E. Regulation of bovine glutamate dehydrogenase. The effects of pH and ADP. *Journal of Biological Chemistry* **1982**, *257*, 5579-5583, doi:10.1016/s0021-9258(19)83816-4.
10. Couée, I.; Tipton, K.F. Activation of glutamate dehydrogenase by l-leucine. *Biochimica et Biophysica Acta (BBA) - Protein Structure and Molecular Enzymology* **1989**, *995*, 97-101, doi:10.1016/0167-4838(89)90239-2.
11. Mkrtchyan, G.; Aleshin, V.; Parkhomenko, Y.; Kaehne, T.; Di Salvo, M.L.; Parroni, A.; Contestabile, R.; Vovk, A.; Bettendorff, L.; Bunik, V. Molecular mechanisms of the non-coenzyme action of thiamin in brain: biochemical, structural and pathway analysis. *Scientific reports* **2015**, *5*, 12583, doi:10.1038/srep12583.
12. Borgnia, M.J.; Banerjee, S.; Merk, A.; Matthies, D.; Bartesaghi, A.; Rao, P.; Pierson, J.; Earl, L.A.; Falconieri, V.; Subramaniam, S., et al. Using Cryo-EM to Map Small Ligands on Dynamic Metabolic Enzymes: Studies with Glutamate Dehydrogenase. *Molecular pharmacology* **2016**, *89*, 645-651, doi:10.1124/mol.116.103382.
13. Fan, H.; Wang, B.; Zhang, Y.; Zhu, Y.; Song, B.; Xu, H.; Zhai, Y.; Qiao, M.; Sun, F. A cryo-electron microscopy support film formed by 2D crystals of hydrophobin HFBI. *Nature communications* **2021**, *12*, doi:10.1038/s41467-021-27596-8.
14. Tomita, T.; Kuzuyama, T.; Nishiyama, M. Structural basis for leucine-induced allosteric activation of glutamate dehydrogenase. *The Journal of biological chemistry* **2011**, *286*, 37406-37413, doi:10.1074/jbc.M111.260265.
15. Tomita, T.; Miyazaki, T.; Miyazaki, J.; Kuzuyama, T.; Nishiyama, M. Hetero-oligomeric glutamate dehydrogenase from Thermus thermophilus. *Microbiology* **2010**, *156*, 3801-3813, doi:10.1099/mic.0.042721-0.
16. Tomita, T.; Yin, L.; Nakamura, S.; Kosono, S.; Kuzuyama, T.; Nishiyama, M. Crystal structure of the 2-iminoglutarate-bound complex of glutamate dehydrogenase from Corynebacterium glutamicum. *FEBS letters* **2017**, *591*, 1611-1622, doi:10.1002/1873-3468.12667.
17. Godsora, B.K.J.; Prakash, P.; Punekar, N.S.; Bhaumik, P. Molecular insights into the inhibition of glutamate dehydrogenase by the dicarboxylic acid metabolites. *Proteins: Structure, Function, and Bioinformatics* **2021**, *90*, 810-823, doi:10.1002/prot.26276.
18. Merk, A.; Bartesaghi, A.; Banerjee, S.; Falconieri, V.; Rao, P.; Davis, M.I.; Pragani, R.; Boxer, M.B.; Earl, L.A.; Milne, J.L.S., et al. Breaking Cryo-EM Resolution Barriers to Facilitate Drug Discovery. *Cell* **2016**, *165*, 1698-1707, doi:10.1016/j.cell.2016.05.040.
19. Tomita, T.; Matsushita, H.; Yoshida, A.; Kosono, S.; Yoshida, M.; Kuzuyama, T.; Nishiyama, M.; Galperin, M.Y. Glutamate Dehydrogenase from Thermus thermophilus Is Activated by AMP and Leucine as a Complex with Catalytically Inactive Adenine Phosphoribosyltransferase Homolog. *Journal of bacteriology* **2019**, *201*, doi:10.1128/jb.00710-18.
20. Grzechowiak, M.; Sliwiak, J.; Jaskolski, M.; Ruszkowski, M. Structural Studies of Glutamate Dehydrogenase (Isoform 1) From Arabidopsis thaliana, an Important Enzyme at the Branch-Point Between Carbon and Nitrogen Metabolism. *Frontiers in plant science* **2020**, *11*, doi:10.3389/fpls.2020.00754.
21. Dimovasili, C.; Fadouloglou, V.E.; Kefala, A.; Providaki, M.; Kotsifaki, D.; Kanavouras, K.; Sarrou, I.; Plaitakis, A.; Zaganas, I.; Kokkinidis, M. Crystal structure of glutamate dehydrogenase 2, a positively selected novel human enzyme involved in brain biology and cancer pathophysiology. *Journal of neurochemistry* **2021**, *157*, 802-815, doi:10.1111/jnc.15296.
22. Gohara, D.W.; Di Cera, E. Molecular Mechanisms of Enzyme Activation by Monovalent Cations. *Journal of Biological Chemistry* **2016**, *291*, 20840-20848, doi:10.1074/jbc.R116.737833.
23. Adelstein, S.J.; Vallee, B.L. Zinc in Beef Liver Glutamic Dehydrogenase. *Journal of Biological Chemistry* **1958**, *233*, 589-593, doi:10.1016/s0021-9258(18)64709-x.
24. Wolf, G.; Schmidt, W. Zinc and glutamate dehydrogenase in putative glutamatergic brain structures. *Acta Histochemica* **1983**, *72*, 15-23, doi:10.1016/s0065-1281(83)80004-x.
25. Bailey, J.; Powell, L.; Sinanan, L.; Neal, J.; Li, M.; Smith, T.; Bell, E. A novel mechanism of V-type zinc inhibition of glutamate dehydrogenase results from disruption of subunit interactions necessary for efficient catalysis. *FEBS Journal* **2011**, *278*, 3140-3151, doi:10.1111/j.1742-4658.2011.08240.x.

26. Aleshin, V.A.; Mkrtchyan, G.V.; Kaehne, T.; Graf, A.V.; Maslova, M.V.; Bunik, V.I. Diurnal regulation of the function of the rat brain glutamate dehydrogenase by acetylation and its dependence on thiamine administration. *Journal of neurochemistry* **2020**, *153*, 80-102, doi:10.1111/jnc.14951.
27. Lombard, D.B.; Alt, F.W.; Cheng, H.L.; Bunkenborg, J.; Streeper, R.S.; Mostoslavsky, R.; Kim, J.; Yancopoulos, G.; Valenzuela, D.; Murphy, A., et al. Mammalian Sir2 homolog SIRT3 regulates global mitochondrial lysine acetylation. *Molecular and cellular biology* **2007**, *27*, 8807-8814, doi:10.1128/MCB.01636-07.
28. Lundby, A.; Lage, K.; Weinert, B.T.; Bekker-Jensen, D.B.; Secher, A.; Skovgaard, T.; Kelstrup, C.D.; Dmytriyev, A.; Choudhary, C.; Lundby, C., et al. Proteomic analysis of lysine acetylation sites in rat tissues reveals organ specificity and subcellular patterns. *Cell reports* **2012**, *2*, 419-431, doi:10.1016/j.celrep.2012.07.006.
29. Bettendorff, L.; Nghiêm, H.-O.; Wins, P.; Lakaye, B. A general method for the chemical synthesis of γ-32P-labeled or unlabeled nucleoside 5′-triphosphates and thiamine triphosphate. *Analytical biochemistry* **2003**, *322*, 190-197, doi:10.1016/j.ab.2003.08.013.
30. Weber, P.; Pissis, C.; Navaza, R.; Mechaly, A.E.; Saul, F.; Alzari, P.M.; Haouz, A. High-Throughput Crystallization Pipeline at the Crystallography Core Facility of the Institut Pasteur. *Molecules* **2019**, *24*, doi:10.3390/molecules24244451.
31. Kabsch, W. Xds. *Acta Crystallographica Section D Biological Crystallography* **2010**, *66*, 125-132, doi:10.1107/s0907444909047337.
32. Vonrhein, C.; Flensburg, C.; Keller, P.; Sharff, A.; Smart, O.; Paciorek, W.; Womack, T.; Bricogne, G. Data processing and analysis with theautoPROCtoolbox. *Acta Crystallographica Section D Biological Crystallography* **2011**, *67*, 293-302, doi:10.1107/s0907444911007773.
33. McCoy, A.J.; Grosse-Kunstleve, R.W.; Adams, P.D.; Winn, M.D.; Storoni, L.C.; Read, R.J. Phasercrystallographic software. *Journal of Applied Crystallography* **2007**, *40*, 658-674, doi:10.1107/s0021889807021206.
34. Emsley, P.; Lohkamp, B.; Scott, W.G.; Cowtan, K. Features and development of Coot. *Acta Crystallographica Section D Biological Crystallography* **2010**, *66*, 486-501, doi:10.1107/s0907444910007493.
35. Smart, O.S.; Womack, T.O.; Flensburg, C.; Keller, P.; Paciorek, W.; Sharff, A.; Vonrhein, C.; Bricogne, G. Exploiting structure similarity in refinement: automated NCS and target-structure restraints inBUSTER. *Acta Crystallographica Section D Biological Crystallography* **2012**, *68*, 368-380, doi:10.1107/s0907444911056058.
36. Williams, C.J.; Headd, J.J.; Moriarty, N.W.; Prisant, M.G.; Videau, L.L.; Deis, L.N.; Verma, V.; Keedy, D.A.; Hintze, B.J.; Chen, V.B., et al. MolProbity: More and better reference data for improved all-atom structure validation. *Protein Science* **2018**, *27*, 293-315, doi:10.1002/pro.3330.
37. Liebschner, D.; Afonine, P.V.; Baker, M.L.; Bunkóczi, G.; Chen, V.B.; Croll, T.I.; Hintze, B.; Hung, L.-W.; Jain, S.; McCoy, A.J., et al. Macromolecular structure determination using X-rays, neutrons and electrons: recent developments in Phenix. *Acta Crystallographica Section D Structural Biology* **2019**, *75*, 861-877, doi:10.1107/s2059798319011471.
38. Weiss, M.S. Global indicators of X-ray data quality. *Journal of Applied Crystallography* **2001**, *34*, 130-135, doi:10.1107/s0021889800018227.